Ruthenium half-sandwich complexes as protein kinase inhibitors: derivatization of the pyridocarbazole pharmacophore ligand†

Nicholas Pagano,[a] Jasna Maksimoska,[a] Howard Bregman,[a] Douglas S. Williams,[a] Richard D. Webster,[b] Feng Xue[c] and Eric Meggers*[a]
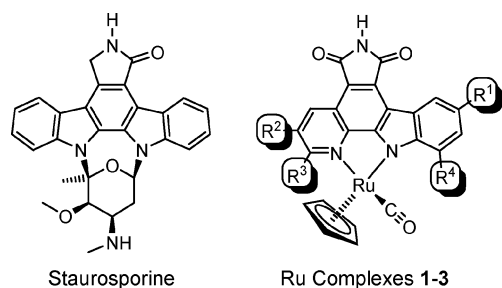
A general route to ruthenium pyridocarbazole half-sandwich complexes is presented and applied to the synthesis of sixteen new compounds, many of which have modulated protein kinase inhibition properties. For example, the incorporation of a fluorine into the pyridine moiety increases the binding affinity for glycogen synthase kinase 3 by almost one order of magnitude. These data are supplemented with cyclic voltammetry experiments and a protein co-crystallographic study.

Introduction

An important objective for the discovery of compounds with new and unique biological activities is the development of methods for the straightforward synthesis of molecular scaffolds with defined three-dimensional shapes. Towards this goal, we recently started a research program that explores the scope of using metal complexes.[1–8] In our concept, structures are built from a metal center with the main function of the metal being to organize the organic ligands in three-dimensional space.

As a proof-of-principle study, we have designed over the last two years organometallic inhibitors for protein kinases by using the class of ATP-competitive indolocarbazole alkaloids (*e.g.* staurosporine,[9] Fig. 1) as a lead structure.[2–8] For this, we replaced the indolocarbazole alkaloid scaffold with simple metal complexes such as **1** and **2** in which the main features of the indolocarbazole aglycon are retained in the metal-chelating pyridocarbazole ligand, whereas the carbohydrate is replaced by a ruthenium fragment. Although structurally related, these new scaffolds turned out to possess properties which are distinct from their parent indolocarbazole alkaloids. For example, whereas staurosporine is a highly unselective protein kinase inhibitor, the half-sandwich compounds **1** and **2** show a remarkable preference for just a few kinases, especially GSK-3 and Pim-1.

In order to modulate the potency and selectivity profiles of organometallics **1** and **2**, as well as their pharmacokinetic properties for future *in vivo* studies, we were interested in functionalizing this scaffold. The pyridocarbazole heterocycle is a main pharmacophore which is designed to bind in the adenine pocket of the ATP binding site and thus constitutes an important target for modifications. Previous synthetic approaches from our group to

	R¹	R²	R³	R⁴
1	H	H	H	H
2	OH	H	H	H
3a	H	F	H	H
3b	H	CF₃	H	H
3c	H	CH₂OH	H	H
3d	H	CH₃	H	H
3e	H	N(CH₃)₂	H	H
3f	H	OCH₃	H	H
3g	H	H	Cl	H
3h	H	H	Br	H
3i	H	H	CH₂OH	H
3j	OH	F	H	H
3k	OH	CF₃	H	H
3l	OH	CH₂OH	H	H
3m	OH	CO₂H	H	H
3n	Cl	H	H	H
3o	Br	H	H	H
3p	OH	H	H	Br

Fig. 1 Staurosporine as a lead structure for functionalized ruthenium pyridocarbazole half-sandwich complexes **1–3**. All complexes are racemic but only the (*S*)-isomer is shown.

derivatize this heterocycle required cumbersome readjustments of the reaction conditions for every new compound.[4,7] We here now report a more general and efficient synthetic strategy for the synthesis of functionalized pyridocarbazole ruthenium compounds, apply it to the synthesis of sixteen new derivatives **3a–p** (Fig. 1), and present preliminary kinase inhibition results and structural data.

[a]Department of Chemistry, University of Pennsylvania, 231 South 34th Street, Philadelphia, PA, 19104, USA. E-mail: meggers@sas.upenn.edu; Fax: +1 215 746 0348; Tel: +1 215 573 1953
[b]Division of Chemistry and Biological Chemistry, Nanyang Technological University, Singapore 637616
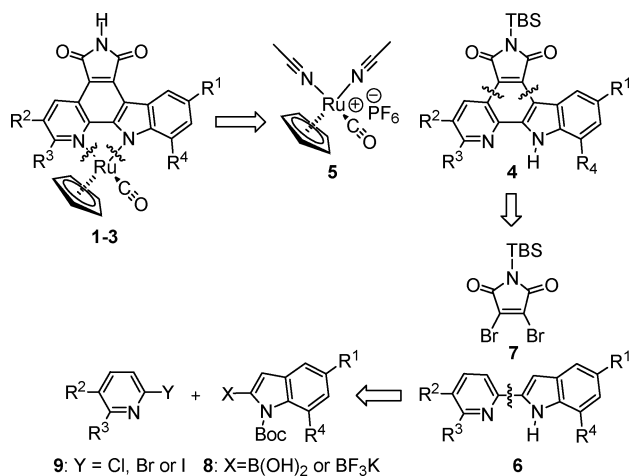[c]Department of Chemistry, National University of Singapore, 3 Science Drive 3, Singapore 117543

Results and discussion

Synthesis

A retrosynthetic analysis of ruthenium complexes **1–3** is shown in Scheme 1. The ruthenium fragment is introduced by reacting a *tert*-butyldimethylsilyl (TBS)-protected pyridocarbazole **4** with the ruthenium half-sandwich complex **5** in the presence of a weak base, followed by TBAF deprotection to afford the ruthenium pyridocarbazoles **1–3**. Thus, the key aspect of a general synthesis is the formation of the TBS-protected pyridocarbazole **4**. Heterocycle **4** can be constructed from the reaction of pyridoindoles **6** with TBS-protected dibromomaleimide **7** by a sequence of substitution and photocyclization.[4] Pyridoindoles are accessible by Suzuki coupling of indole boronic acids **8** or their trifluoroborates with α-halogenated pyridines **9**.[10] Thus, overall, in our new synthetic scheme, ruthenium pyridocarbazoles **1–3** are assembled from four easily accessible building blocks (**5**, **7–9**) in three consecutive C–C bond formation steps followed by a coordination chemistry step. A major improvement of this synthetic scheme over previous ones from our group is the ability to access a large variety of pyridoindoles through a reliable Suzuki coupling instead of Fischer indole synthesis.

Derivatives of indole **8** were prepared in two or three synthetic steps from the appropriate commercially available indoles **10a** and **10b** by Boc-protection to **11a** and **11b**, followed by introducing the boronic acid to **8a** and **8b** (Scheme 2).[11] These boronic acids can then optionally be transformed into the crystalline trifluoroborates **8c** and **8d** by reaction with KHF$_2$.[12] The trifluoroborates **8c** and **8d** are much more stable compared to **8a** and **8b** and can simply be stored on the bench. In addition, as discussed below, they afford significantly higher yields in the Suzuki coupling with α-halogenated pyridines.

Scheme 2 Synthesis of the indole building block **8**.
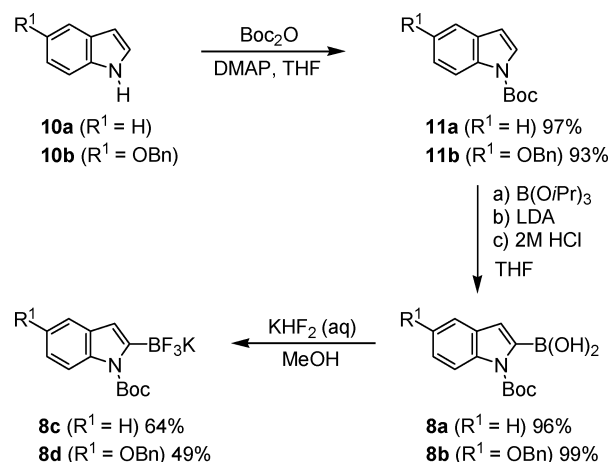
Subsequent Suzuki cross-coupling of indoles **8a–d** with α-halogenated pyridines **9a–j** furnished pyridoindoles with the Boc-protection group partially removed. Unable to easily separate the two compounds in most cases, the purified mixtures in each case were adsorbed onto silica gel and heated under high vacuum to afford pyridoindoles **6a–m** (Table 1).[13] Reaction yields were in the range of 47–91% over the two steps. In general, good to excellent

Scheme 1 Retrosynthetic analysis of **1–3**.

Table 1 Pyridoindole synthesis by Suzuki coupling[a]

Entry	Pyridine (R^2, R^3, Y)		Indole	Pyridoindole (R^1, R^2, R^3)		Yield (%)
1	**9a**	F, H, Br	**8a**	**6a**	H, F, H	62
2	**9b**	CF$_3$, H, Cl	**8a**	**6b**	H, CF$_3$, H	57
3	**9c**	CH$_2$OTBS, H, Br	**8a**	**6c**	H, CH$_2$OTBS, H	84
4	**9d**	CH$_3$, H, Br	**8c**	**6d**	H, CH$_3$, H	91
5	**9e**	N(CH$_3$)$_2$, H, Br	**8c**	**6e**	H, N(CH$_3$)$_2$, H	86
6	**9f**	OCH$_3$, H, Br	**8c**	**6f**	H, OCH$_3$, H	85
7	**9g**	H, Cl, I	**8a**	**6g**	H, H, Cl	66
8	**9h**	H, Br, I	**8a**	**6h**	H, H, Br	52
9	**9i**	H, CH$_2$OTBS, Br	**8a**	**6i**	H, H, CH$_2$OTBS	67
10	**9a**	F, H, Br	**8b** (**8d**)	**6j**	OBn, F, H	57 (87)[b]
11	**9b**	CF$_3$, H, Cl	**8b** (**8d**)	**6k**	OBn, CF$_3$, H	52 (73)[b]
12	**9c**	CH$_2$OTBS, H, Br	**8b**	**6l**	OBn, CH$_2$OTBS, H	68
13[c]	**9j**	CO$_2$Z, H, Br	**8b**	**6m**	OBn, CO$_2$Z, H	47

[a] Reaction conditions: first, 1.1 equiv of **8a–d**, 1.0 equiv **9a–j**, 0.1 equiv of Pd(0) or Pd(II) catalyst, 2.75 equiv Na$_2$CO$_3$, DME–H$_2$O, reflux, overnight, then 10 : 1 mass ratio silica gel : indole, high vacuum, 80 °C, overnight. [b] Yields with trifluoroborate **8d**. [c] Z = CH$_2$CH$_2$Si(CH$_3$)$_3$.

This journal is © The Royal Society of Chemistry 2007

Org. Biomol. Chem., 2007, **5**, 1218–1227 | 1219

yields were observed when using the potassium trifluoroborates **8c** and **8d** as the indole coupling partner. This difference can be attributed to a suppressed formation of a bis-indole homocoupling product which is present when using boronic acids **8a** and **8b**. From these studies we can conclude that the synthesis of pyridoindoles through Suzuki coupling with trifluoroborates is superior to the more traditional Fischer indole synthesis with respect to generality and accessibility of a wide variety of derivatives.

For the following reaction with TBS-protected dibromomaleimide **7**, the benzyl-protection group located on pyridoindoles **6j–m** was first replaced by a TBS group in order to simplify a later deprotection (Scheme 3). This was accomplished by hydrogenolysis with H_2, Pd/C furnishing the phenol derivatives **12j–m**, followed by the treatment with TBS-triflate in presence of the base di(isopropyl)ethylamine to afford the TBS-protected pyridoindoles **13j–m**.
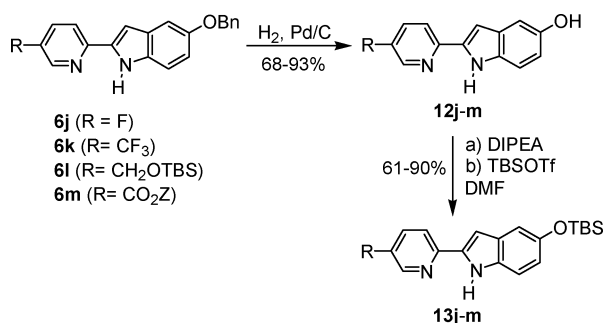
Scheme 3 Protection group exchange of pyridoindoles **6j–m** to **13j–m**.

For the next two C–C bond formations, pyridoindoles **6a-i** and **13j–m** were condensed with dibromomaleimide **7** as shown in Scheme 4. This method was successfully used by Murase *et al.* for the synthesis of granulatimides and their analogs.[4,14] Accordingly, pyridoindoles **6a–i** and **13j–m** were treated with at least two equivalents of LiHMDS and quenched with TBS-protected dibromomaleimide **7**, furnishing the relatively unstable monobromides **14a–m** in yields of 34–78%. As a trend, reactions involving pyridoindoles bearing only electron-withdrawing groups on the pyridine were sluggish (**14a**, **14b**, **14g**, and **14h**), likely as a result of the decreased nucleophilicity of the joined heterocycles.

Cyclization of the monobromide intermediates **14a–m** by an anaerobic photocyclization with a medium pressure Hg lamp using an uranium filter (50% transmission at 350 nm) yielded the corresponding pyridocarbazoles **4a–m**. In the course of the photocyclization, the solubility decreases significantly and the compounds generally precipitate out. The major side product of this reaction was found in the competing cyclization by substituting the bromide with the pyridine nitrogen, leading to pyridinium salts. This competing salt formation can be influenced by steric effects and the polarity of the solvent. For example, the monobromides **14g**, **14h** and **14i** undergo photocyclization in outstanding yields (86–96%) and it is likely that substitution at the 2-position of the pyridine heterocycle precludes the formation of a pyridinium bromide salt due to steric hindrance of the pyridine nitrogen. Yields also improve significantly by using a less polar solvent such as toluene which appears to disfavor the transition state of the salt side product.
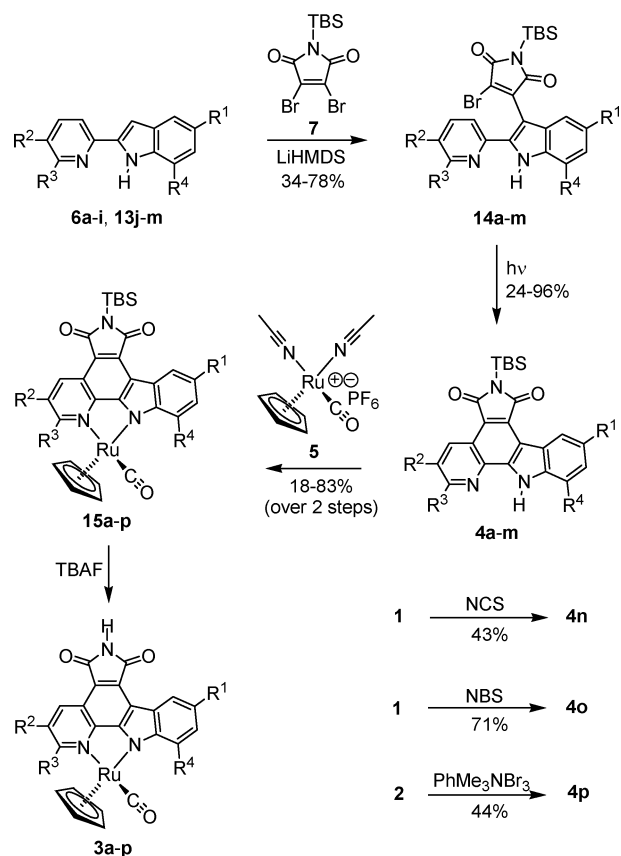

Scheme 4 Assignments of R^1–R^4: see Fig. 1 for compounds **3a–p**. For all intermediates, see Table 1 (**a–i** and **n–p**) and Scheme 3 (**j–m**).

The pyridocarbazoles **4** can now further become functionalized after their assembly. For example, our group has had some success in directly functionalizing the pyridocarbazole ligands **1** and **2** utilizing electrophilic aromatic substitution reactions.[7] In the absence of previously existing functionality at the indole moiety, both chlorination product **4n** and bromination product **4o** were isolated with exclusive addition to the 5-position of the indole heterocycle, by reaction with NCS and NBS, respectively (Scheme 4). In the case where this position at the indole is already occupied, addition was directed towards the 7-position of the indole. We have previously reported the bromination of **2** to afford the disubstituted product **4p** by reaction with $PhMe_3NBr_3$ (Scheme 4).[7]

Finally, the reaction of each pyridocarbazole ligand **4** with the common ruthenium precursor **5** furnishes TBS-protected organometallic complexes **15–p**. Despite the uncommon involvement of an indole, the heterocycles **4** are reliable coordinating ligands which lose a proton upon introduction into the coordination sphere of a metal. However, reactions with pyridocarbazoles bearing substitutions at the 2-position of the pyridine (**4g–i**) are sluggish, likely because they sterically interfere with complex formation. It is also noteworthy that the TBS group in the heterocycles **4** is necessary in order to increase the solubility of the ligands in organic solvents. Ten of the sixteen complexes were isolated and desilylated in a separate synthetic step, while the remaining six were desilylated *in situ* providing the final organometallic inhibitors **3a–p**.

Protein kinase inhibition and cyclic voltammetry

Screening data for these new compounds at a single concentration against the protein kinase GSK-3 and Pim-1 are displayed in Fig. 2. These data demonstrate that derivatizations of the indole and/or pyridine moiety lead to significant modulations in inhibition potencies and selectivities. Although compounds **3g**, **3h**, **3n**, and **3o** display similar or reduced potencies compared to **1**, all remaining compounds are modestly or significantly improved inhibitors for GSK-3 and Pim-1. Importantly, substituents also influence the kinase selectivities. Whereas compound **3m** strongly prefers Pim-1, **3p** instead possesses a switched selectivity towards GSK-3 as has been demonstrated previously.[7]
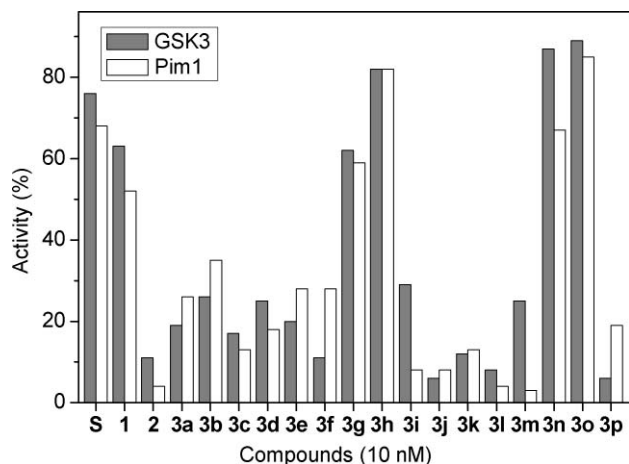

Fig. 2 Screening of ruthenium complexes **1**–**3** against GSK-3 and Pim-1 at a concentration of 10 nM. Staurosporine (**S**) was used as a reference.

Fig. 2 also reveals that all synthesized modifications at the *meta*-position of the pyridine moiety (R^2) are beneficial for the inhibition of GSK-3 and Pim-1 (**3a**–**f**). Especially interestingly, adding a single fluorine (**3a**) increases the binding to GSK-3 significantly. The concentration at which 50% of the kinase is inhibited (IC_{50}) was determined to be 2.5 nM for **3a** at 100 µM ATP, which is a decrease by almost one order of magnitude just by exchanging a single hydrogen for a fluorine (Fig. 3).

In addition, as has been observed before and can also be extracted from the screening data in Fig. 2, an OH group at the indole R^1 position generally increases the affinity of compounds significantly (see **2**, **3j**–**m**, and **3p**).[3] However, it is noteworthy that the OH group poses a potential risk in terms of enzymatic or chemical oxidation in a biological environment. For example, a comparison of cyclic voltammetry data for compounds **1** and **2** reveals that the addition of an OH group into the indole moiety (**2**) results in an oxidative peak potential which is *ca.* 0.18 V lower as compared to **1**. Furthermore, whereas the oxidation of **1** is chemically reversible at a scan rate of 1 V s^{-1} at 293 K, compound **2** displays complicated oxidative electrochemistry and appears to decompose/react after initial oxidation (data not shown). In contrast to the OH group in **2**, the fluorine moiety in **3a** increases the resistance to (chemically reversible) oxidation, yielding an oxidative peak potential that is 0.06 V higher compared to **1**.

From all these data it can be concluded that a fluorine substituent at the *meta*-position of the pyridine moiety (R^2) as in **3a** offers a promising compromise between affinity and
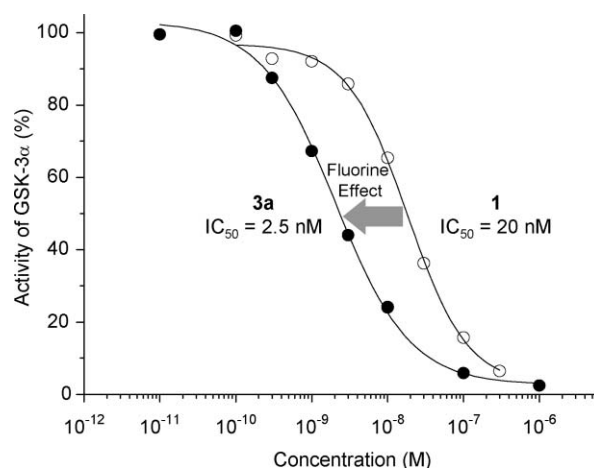
Fig. 3 IC_{50} curves of compounds **1** and **3a** against GSK-3 (α-isoform) demonstrating the effect of substituting one hydrogen against fluorine. The ATP concentration was 100 µM.
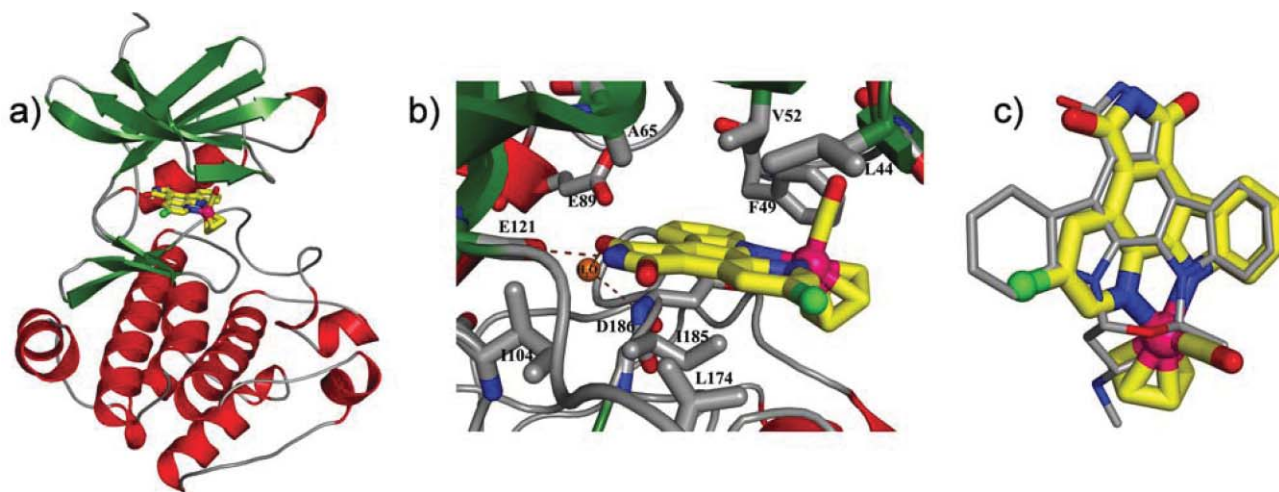
chemical robustness for the design of GSK-3 inhibitors to be used as molecular probes for signaling pathways involving GSK-3. Improving selectivities, especially with respect to Pim-1, can be accomplished in future work by additional modifications at the cyclopentadienyl moiety as has been demonstrated recently.[8]

Cocrystal structure of (*S*)-3a with Pim-1

We succeeded in cocrystallizing full-length human Pim-1 with the enantiomer (*S*)-**3a** and solved the structure to a resolution of 2.2 Å.[15] This structure is related to previous Pim-1 cocrystal structures with (*R*)-**1** and (*S*)-**2**.[6] Fig. 4 demonstrates that the ruthenium complex occupies the ATP binding site of the protein kinase.[16] The pyridocarbazole moiety of (*S*)-**3a** is nicely placed inside the hydrophobic pocket formed by Leu44, Phe49, Val52, as well as Ala65 of the N-terminal domain, and Ile104, Val126, Leu174, and Ile185 of the C-terminal domain. In agreement with the initial design, (*S*)-**3a** retains the hydrogen bonding pattern of ATP by forming one characteristic hydrogen bond between the imide NH group and the backbone carbonyl oxygen atom of Glu121 within the hinge region. An additional water mediated hydrogen bond is established between the maleimide group of (*S*)-**3a** and Asp186 (Fig. 4b). The CO group points towards the glycine rich loop and the cyclopentadienyl moiety packs against Phe49 and Ile185, while the fluorine substituent points towards the solvent without having any notable contact. The improved binding affinity by introducing a fluorine (**1** → **3a**) may be due to a subtle dipole effect.

Intriguingly, superposition of the binding positions of cocrystallized (*S*)-**3a** and staurosporine (PDB code 1YHS) with Pim-1 demonstrates how closely the ruthenium complex mimics the binding mode of staurosporine.[17] The pyridocarbazole ligand perfectly mimics the position of the indolocarbazole moiety of staurosporine while the cyclopentadienyl ring and the CO group occupy the binding position of the carbohydrate moiety of staurosporine (Fig. 4c). Importantly, the ruthenium center is not involved in any direct interaction and has solely a structural role.

This journal is © The Royal Society of Chemistry 2007

Org. Biomol. Chem., 2007, **5**, 1218–1227 | 1221

Fig. 4 Cocrystal structure of (*S*)-**3a** with Pim-1 at 2.2 Å. a) The ruthenium complex occupies the ATP binding site of Pim-1. b) The most important interactions between (*S*)-**3a** and Pim-1. c) Superimposed relative binding positions of (*S*)-**3a** staurosporine to Pim-1 (PDB code 1YHS).

Conclusions

We have developed an efficient and general strategy for the synthesis of modified pyridocarbazoles in ruthenium half-sandwich kinase inhibitors. Preliminary kinase inhibition results demonstrate that these modifications have a significant effect on the kinase inhibition profiles. Future work will combine functionalizations at the pyridocarbazole moiety with a derivatization at the cyclopentadienyl moiety in order to generate GSK-3 and Pim-1 inhibitors with improved selectivities and potencies, as well as hopefully favorable *in vivo* properties.

Experimental

Synthesis

The exemplary complete syntheses of the fluorinated compounds **3a** and **3j** are described. See ESI† for all other compounds. Reactions were carried out using oven-dried glassware and were conducted under a positive pressure of argon unless otherwise specified. NMR spectra were recorded on a DMX-360 (360 MHz) or Bruker AM-500 (500 MHz) spectrometer. Infrared spectra were recorded on a Perkin-Elmer 1600 series FTIR spectrometer. Low-resolution mass spectra were obtained on an LC platform from Micromass using the ESI technique. ES-TOF spectra were measured by Waters Micromass MS Technologies. High-resolution mass spectra were obtained with a Micromass AutoSpec instrument using either CI or ES ionization. Reagents and solvents were used as received from standard suppliers. Chromatographic separations were performed using Silia-P Flash silica gel from Silicycle Inc.

Compound 11b. A solution of **10b** (5.0 g, 22.4 mmol) in THF (16.5 mL) was purged with argon while cooling to 0 °C. To the solution was added di-*tert*-butyl dicarbonate (5.4 mL, 23.5 mmol) followed by the careful addition of solid (dimethylamino)pyridine (DMAP) (4.1 g, 33.6 mmol). Upon complete addition of DMAP, the reaction mixture quickly solidified and the resulting white solid was gently warmed until it began to bubble. The resulting white suspension was stirred at room temperature overnight. The reaction mixture was cooled to 0 °C and 1 M HCl (12.5 mL)

was carefully added. After stirring at room temperature for 5 minutes, the organic layer was separated and the aqueous layer was extracted with EtOAc. The combined organic layers were washed with brine, dried using Na_2SO_4, filtered and concentrated to dryness *in vacuo*. The crude material was adsorbed onto silica gel and subjected to silica gel chromatography with hexanes–EtOAc (15 : 1). The combined product eluents were dried *in vacuo* to provide **11b** (6.6 g, 93%) as a white solid. ¹H NMR (360 MHz, DMSO-d_6): δ (ppm) 7.92 (d, $J = 9.0$ Hz, 1H), 7.61 (d, $J = 3.7$ Hz, 1H), 7.46–7.31 (m, 5H), 7.21 (d, $J = 2.5$ Hz, 1H), 7.00 (dd, $J = 9.0, 2.5$ Hz, 1H), 6.61 (d, $J = 3.7$ Hz, 1H), 5.12 (s, 2H), 1.60 (s, 9H). ¹³C NMR (90 MHz, DMSO-d_6): δ (ppm) 154.9, 149.5, 137.7, 131.5, 129.7, 128.8, 128.2, 128.1, 127.1, 115.8, 114.1, 107.8, 105.4, 84.0, 70.0, 28.1. IR (film): v (cm⁻¹) 2981, 2928, 1730, 1611, 1585, 1470, 1453, 1374, 1347, 1334, 1286, 1268, 1163, 1150, 1119, 1083, 1018, 846, 807. HRMS calcd for $C_{20}H_{21}NO_3$ (M)⁺ 323.1521, found (M)⁺ 323.1533.

Compound 8b. A solution of **11b** (6.0 g, 18.6 mmol) in anhydrous THF (24 mL) was prepared after drying **11b** overnight under high vacuum. Following the addition of triisopropyl borate (6.5 mL, 28.0 mmol), the reaction mixture was cooled to 0 °C and lithium diisopropylamide (2.0 M solution in heptane–tetrahydrofuran–ethylbenzene) (14 mL, 28.0 mmol) was added dropwise over 1 hour. After stirring for an additional 30 minutes at 0 °C, 2 M HCl (50 mL) was carefully added and allowed to stir at room temperature for 10 minutes. The resulting layers were separated and the aqueous layer was extracted using EtOAc. The combined organic layers were dried using Na_2SO_4, filtered and concentrated to dryness *in vacuo* to provide **8b** (6.7 g, 99%) as a tan solid. Attempts to further purify the crude material by column chromatography resulted in significant decomposition of **8b**.

Compound 8c. A solution of **8a** (24.0 g, 92.2 mmol) in MeOH (300 mL) was purged with argon while cooling to 0 °C. A saturated solution of potassium hydrogen fluoride (82.0 mL) was slowly added and the resulting thick suspension was stirred at room temperature for 4 hours. The light orange suspension was evaporated to dryness *in vacuo* and dried under high vacuum overnight to remove all residual water. To the resulting light

orange solid was added acetone (750 mL), and the suspension was stirred at 40 °C for approximately 30 minutes. Any undissolved material (inorganic salts) was removed by filtration and the filtrate was concentrated to dryness *in vacuo*. The crude material was redissolved in a minimal amount of acetone and the product was precipitated with addition of ether. Collection of the precipitate by filtration provided **8c** (19.1 g, 64%) as white crystals. ^{1}H NMR (500 MHz, acetone-d_6): δ (ppm) 8.01 (d, $J = 8.0$ Hz, 1H), 7.39 (m, 1H), 7.09 (ddd, $J = 8.4, 7.0, 1.4$ Hz, 1H), 7.05 (td, $J = 7.3, 1.2$ Hz, 1H), 6.64 (s, 1H), 1.67 (s, 9H). ^{13}C NMR (125 MHz, acetone-d_6): δ (ppm) 152.5, 138.7, 132.6, 122.8, 122.3, 120.4, 116.3, 113.9, 83.0, 28.5 (C–B not observed). IR (film): ν (cm^{-1}) 3414, 2974, 1730, 1637, 1450, 1369, 1330, 1251, 1214, 1153, 1121, 983, 892, 847, 746. HRMS calcd for $C_{13}H_{14}BF_3NO_2$ (M)$^-$ 284.1070, found (M)$^-$ 284.1073.

Compound 8d. A solution of **8b** (16.0 g, 43.6 mmol) in MeOH (240 mL) was purged with argon while cooling to 0 °C. A saturated solution of potassium hydrogen fluoride (38.8 mL) was slowly added and the resulting thick suspension was stirred at room temperature for 6 hours. The light orange suspension was evaporated to dryness *in vacuo* and dried under high vacuum overnight to remove all residual water. To the resulting light orange solid was added acetone (560 mL), and the suspension was stirred at 40 °C for approximately 1 hour. Any undissolved material (inorganic salts) was removed by filtration and the filtrate was concentrated to dryness *in vacuo*. The crude material was redissolved in a minimal amount of acetone and the product was precipitated with addition of ether. Collection of the precipitate by filtration provided **8d** (9.16 g, 49%) as a white solid. ^{1}H NMR (500 MHz, acetone-d_6): δ (ppm) 7.91 (d, $J = 9.0$ Hz, 1H), 7.50–7.29 (m, 5H), 7.03 (d, $J = 2.5$ Hz, 1H), 6.80 (dd, $J = 9.0, 2.6$ Hz, 1H), 6.56 (s, 1H), 5.12 (s, 2H), 1.66 (s, 9H). ^{13}C NMR (125 MHz, acetone-d_6): δ (ppm) 155.4, 152.4, 139.2, 133.7, 133.5, 129.2, 128.4, 116.8, 113.8, 111.9, 104.7, 104.6, 82.7, 70.9, 28.5 (C–B not observed). IR (film): ν (cm^{-1}) 2975, 2870, 1721, 1615, 1544, 1450, 1372, 1327, 1253, 1187, 1158, 1128, 1096, 988, 869. HRMS calcd for $C_{20}H_{20}BF_3NO_3$ (M)$^-$ 390.1488, found (M)$^-$ 390.1487.

Compound 6a. A biphasic suspension of **8a** (6.50 g, 25.0 mmol), **9a** (4.00 g, 22.7 mmol), tetrakis(triphenylphosphine)-palladium(0) (2.62 g, 2.27 mmol) and Na$_2$CO$_3$ (6.62 g, 62.4 mmol) in 1,2-dimethoxyethane (227 mL) and water (25 mL) was purged with argon and refluxed overnight. The resulting orange reaction mixture was cooled to room temperature, diluted with water and extracted with EtOAc. The combined organic layers were washed with brine, dried using Na$_2$SO$_4$, filtered and concentrated to dryness *in vacuo*. The crude material was adsorbed onto silica gel and subjected to silica gel chromatography with hexanes–EtOAc (15 : 1 to 10 : 1). The combined product eluents were isolated as a mixture of Boc-protected pyridoindole and **6a**. The resulting white solid (4.5 g) was dissolved into CH$_2$Cl$_2$ and adsorbed onto silica gel (45.0 g) using rotary evaporation. The white powder was heated to 80 °C overnight under high vacuum. The silica gel was cooled to room temperature, filtered through celite with EtOAc and the filtrate concentrated to dryness *in vacuo*. The crude material was adsorbed onto silica gel and subjected to silica gel chromatography with hexanes–EtOAc (10 : 1). The combined product eluents were dried *in vacuo* to provide **6a** (3.00 g, 62% over two steps) as a white

solid. ^{1}H NMR (360 MHz, CDCl$_3$): δ (ppm) 9.45 (s, 1H), 8.44 (d, $J = 2.8$ Hz, 1H), 7.79 (ddd, $J = 8.8, 4.3, 0.6$, 1H), 7.66 (dd, $J = 7.9, 0.9$ Hz, 1H), 7.43 (m, 2H), 7.23 (ddd, $J = 8.2, 7.0, 1.2$ Hz, 1H), 7.13 (ddd, $J = 8.0, 7.0, 1.0$ Hz, 1H), 6.96 (dd, $J = 2.0, 0.8$ Hz, 1H). ^{13}C NMR (90 MHz, CDCl$_3$): δ (ppm) 158.8 (d$_{C-F}$, $J = 255.5$ Hz), 147.1 (d$_{C-F}$, $J = 4.0$ Hz), 137.4, (d$_{C-F}$, $J = 24.4$ Hz), 136.7, 136.1, 129.3, 124.0 (d$_{C-F}$, $J = 19.1$ Hz), 123.5, 121.4, 120.9 (d$_{C-F}$, $J = 4.4$ Hz), 120.5, 111.5, 100.5. IR (film): ν (cm^{-1}) 3424, 3056, 1597, 1549, 1467, 1449, 1425, 1376, 1350, 1302, 1263, 1230, 1116, 1046, 1010, 933, 909, 837, 798, 742. HRMS calcd for $C_{13}H_9FN_2$ (M)$^+$ 212.0750, found (M)$^+$ 212.0753.

Compound 6j using 8b. A biphasic suspension of **8b** (2.87 g, 7.82 mmol), **9a** (1.25 g, 7.10 mmol), bis(triphenyl-phosphine)palladium(II) chloride (500 mg, 0.71 mmol) and 2 M Na$_2$CO$_3$ (40 mL) in 1,2-dimethoxyethane (72 mL) and water (8 mL) was purged with argon and refluxed overnight. The reaction mixture was cooled to room temperature, diluted with water and extracted with EtOAc. The combined organic layers were washed with brine, dried using Na$_2$SO$_4$, filtered and concentrated to dryness *in vacuo*. The crude material was adsorbed onto silica gel and subjected to silica gel chromatography with hexanes–EtOAc (10 : 1). The combined product eluents were isolated as a mixture of Boc-protected pyridoindole and **6j**. The resulting white solid (1.82 g) was dissolved into CH$_2$Cl$_2$ and adsorbed onto silica gel (18.2 g) using rotary evaporation. The white powder was heated to 80 °C overnight under high vacuum. The silica gel was cooled to room temperature, filtered through celite with EtOAc and the filtrate dried *in vacuo* to provide **6j** (1.28 g, 57% over two steps) as a white solid. ^{1}H NMR (360 MHz, CDCl$_3$): δ (ppm) 9.35 (s, 1H), 8.41 (d, $J = 2.8$ Hz, 1H), 7.75 (dd, $J = 8.8, 4.3$, 1H), 7.50–7.30 (m, 7H), 7.16 (d, $J = 2.4$ Hz, 1H), 6.98 (dd, $J = 8.8, 2.4$ Hz, 1H), 6.87 (d, $J = 1.9$ Hz, 1H), 5.12 (s, 2H). ^{13}C NMR (90 MHz, CDCl$_3$): δ (ppm) 158.7 (d$_{C-F}$, $J = 255.7$ Hz) 153.9, 147.1 (d$_{C-F}$, $J = 3.8$ Hz), 137.9, 137.4 (d$_{C-F}$, $J = 24.4$ Hz), 136.7, 132.3, 129.7, 128.7, 128.0, 127.8, 124.0 (d$_{C-F}$, $J = 19.2$ Hz), 120.8 (d$_{C-F}$, $J = 4.3$ Hz), 114.8, 112.3, 104.4, 100.3, 71.1. IR (film): ν (cm^{-1}) 3438, 3095, 3051, 3025, 2884, 2849, 1598, 1549, 1462, 1448, 1422, 1374, 1347, 1290, 1264, 1228, 1207, 1158, 1114, 1035, 956, 934, 916, 837. HRMS calcd for $C_{20}H_{15}FN_2O$ (M)$^+$ 318.1168, found (M)$^+$ 318.1183.

Compound 6j using 8d. A biphasic suspension of **8d** (268 mg, 0.625 mmol), **9a** (100 mg, 0.568 mmol), tetrakis(triphenyl-phosphine)palladium(0) (66 mg, 0.057 mmol) and Na$_2$CO$_3$ (165 mg, 1.56 mmol) in 1,2-dimethoxyethane (2.5 mL) and water (0.73 mL) was purged with argon and refluxed overnight. The resulting yellow reaction mixture was cooled to room temperature, diluted with water and extracted with EtOAc. The combined organic layers were washed with brine, dried using Na$_2$SO$_4$, filtered and concentrated to dryness *in vacuo*. The crude material was adsorbed onto silica gel and subjected to silica gel chromatography with hexanes–EtOAc (8 : 1). The combined product eluents were isolated as a mixture of Boc-protected pyridoindole and **6j**. The resulting white solid (209 mg) was dissolved into EtOAc and adsorbed onto silica gel (2.09 g) using rotary evaporation. The white powder was heated to 80 °C overnight under high vacuum. The silica gel was cooled to room temperature, filtered through celite with EtOAc and the filtrate dried *in vacuo* to provide **6j** (158 mg, 87% over two steps) as a white solid.

This journal is © The Royal Society of Chemistry 2007

Org. Biomol. Chem., 2007, **5**, 1218–1227 | 1223

Compound 12j. A suspension of **6j** (1.22 g, 3.84 mmol) in ethanol (80 mL) was purged with argon for 15 minutes. Following thorough argon purge, palladium (10 wt% on activated carbon, wet, Degussa type E101 NE/W) (1.22 g) was added and the reaction mixture was carefully purged with hydrogen gas and stirred at room temperature under an atmosphere of hydrogen for 5 hours. The resulting dark blue reaction mixture was filtered through celite with EtOAc and the filtrate concentrated to dryness *in vacuo*. The crude material was subjected to silica gel chromatography with hexanes–EtOAc (3 : 1 to 1 : 1). The combined product eluents were dried *in vacuo* to provide **12j** (720 mg, 82%) as a yellow solid. ^{1}H NMR (360 MHz, DMSO-d_6): δ (ppm) 11.31 (s, 1H), 8.69 (s, 1H), 8.57 (d, J = 2.8 Hz, 1H), 7.97 (dd, J = 8.9, 4.4 Hz, 1H), 7.77 (td, J = 8.8, 2.9 Hz, 1H), 7.24 (d, J = 8.7 Hz, 1H), 6.91 (s, 1H), 6.85 (d, J = 2.0 Hz, 1H), 6.65 (dd, J = 8.7, 2.2 Hz, 1H). ^{13}C NMR (90 MHz, DMSO-d_6): δ (ppm) 158.0 (d_{C-F}, J = 252.9 Hz), 151.1, 147.5 (d_{C-F}, J = 3.6 Hz), 137.0 (d_{C-F}, J = 23.9 Hz), 136.5, 132.0, 129.1, 124.2 (d_{C-F}, J = 18.9 Hz), 121.0 (d_{C-F}, J = 4.4 Hz), 113.2, 112.4, 104.0, 99.9. IR (film): ν (cm^{-1}) 3406, 3365, 2545, 1700, 1624, 1579, 1548, 1447, 1427, 1366, 1229, 1148, 1118, 1011, 951, 915, 839, 814, 794, 753, 733. HRMS calcd for $C_{13}H_9FN_2O$ (M)$^+$ 228.0699, found (M)$^+$ 228.0698.

Compound 13j. A solution of **12j** (475 mg, 2.08 mmol) in DMF (7.5 mL) was cooled to 0 °C and *N,N*-diisopropylethylamine (1.81 mL, 10.4 mmol) was added dropwise. After stirring for 10 minutes at 0 °C, *tert*-butyldimethylsilyl trifluoromethanesulfonate (524 µL, 2.29 mmol) was added dropwise over 15 minutes and the reaction mixture was stirred at room temperature for an additional hour. The resulting yellow solution was cooled to 0 °C and 1 M NH$_4$OAc (10 mL) was carefully added. The mixture was then diluted with water and extracted with CH$_2$Cl$_2$. The combined organic layers were dried using Na$_2$SO$_4$, filtered and concentrated to dryness *in vacuo*. The crude material was adsorbed onto silica gel and subjected to silica gel chromatography with hexanes–EtOAc (10 : 1). The combined product eluents were dried *in vacuo* to provide **13j** (640 mg, 90%) as a white solid. ^{1}H NMR (360 MHz, CDCl$_3$): δ (ppm) 9.29 (s, 1H), 8.41 (d, J = 2.9 Hz, 1H), 7.74 (ddd, J = 8.8, 4.3, 0.6, 1H), 7.43 (ddd, J = 8.8, 8.1, 2.9, 1H), 7.24 (dt, J = 8.7, 0.7, 1H), 7.06 (dd, J = 1.7, 0.6 Hz, 1H), 6.83 (dd, J = 2.1, 0.8 Hz, 1H), 6.80 (dd, J = 8.7, 2.3 Hz, 1H), 1.02 (s, 9H), 0.22 (s, 6H). ^{13}C NMR (90 MHz, CDCl$_3$): δ (ppm) 158.7 (d_{C-F}, J = 255.6 Hz), 149.9, 147.1 (d_{C-F}, J = 4.0 Hz), 137.4 (d_{C-F}, J = 24.1 Hz), 136.7, 132.5, 130.0, 124.0 (d_{C-F}, J = 19.2 Hz), 120.8 (d_{C-F}, J = 4.4 Hz), 118.0, 111.9, 110.5, 100.1, 26.0, 18.5, −4.2. IR (film): ν (cm^{-1}) 3415, 3050, 2947, 2928, 2894, 2859, 1621, 1594, 1575, 1550, 1462, 1448, 1427, 1382, 1362, 1317, 1288, 1255, 1239, 1151, 1117, 1009, 965, 938, 924, 890, 862, 837, 792, 779, 754, 738, 718. HRMS calcd for $C_{19}H_{24}FN_2OSi$ (M + H)$^+$ 343.1642, found (M + H)$^+$ 343.1653.

Compound 14a. A solution of **6a** (800 mg, 3.77 mmol) in THF (9.5 mL) was prepared after drying **6a** under high vacuum. After cooling the solution to −15 °C, lithium bis(trimethylsilyl)amide (1 M solution in hexanes) (11.3 mL, 11.3 mmol) was added dropwise over 15 minutes and the resulting yellow suspension was stirred at −15 °C for an additional 45 minutes. A solution of **7** (1.46 g, 3.96 mmol) in THF (9.5 mL) cooled to 0 °C was added and the reaction mixture was stirred at −15 °C for 20 minutes and

room temperature overnight. The resulting dark purple reaction mixture was carefully poured into stirring ice cold 10% HCl (100 mL) and extracted with EtOAc. The combined organic layers were washed with saturated NaHCO$_3$ followed by brine, dried using Na$_2$SO$_4$, filtered and concentrated to dryness *in vacuo*. The crude material was adsorbed onto silica gel and subjected to silica gel chromatography with hexanes–EtOAc (6 : 1). The combined product eluents were dried *in vacuo* to provide **14a** (880 mg, 47%) as an orange solid. The unstable material was immediately subjected to the photocyclization step.

Compound 14j. A solution of **13j** (525 mg, 1.54 mmol) in THF (4.0 mL) was prepared after drying **13j** under high vacuum. After cooling the solution to −15 °C, lithium bis(trimethylsilyl)amide (1 M solution in hexanes) (4.62 mL, 4.62 mmol) was added dropwise over 15 minutes and the resulting red suspension was stirred at −15 °C for an additional 45 minutes. A solution of **7** (598 mg, 1.62 mmol) in THF (4.0 mL) cooled to 0 °C was added and the reaction mixture was stirred at −15 °C for 20 minutes and room temperature overnight. The resulting dark purple reaction mixture was carefully poured into stirring ice cold 10% HCl (50 mL) and extracted with EtOAc. The combined organic layers were washed with saturated NaHCO$_3$ followed by brine, dried using Na$_2$SO$_4$, filtered and concentrated to dryness *in vacuo*. The crude material was adsorbed onto silica gel and subjected to silica gel chromatography with hexanes–EtOAc (6 : 1 to 4 : 1). The combined product eluents were dried *in vacuo* to provide **14j** (620 mg, 64%) as an orange solid. ^{1}H NMR (360 MHz, CDCl$_3$): δ (ppm) 9.65 (s, 1H), 8.44 (s, 1H), 7.26 (m, 3H), 6.94 (d, J = 2.0, 1H), 6.84 (dd, J = 8.7, 2.1, 1H), 1.01 (s, 18H), 0.49 (s, 6H), 0.22 (s, 6H). ^{13}C NMR (90 MHz, CDCl$_3$): δ (ppm) 173.5, 171.0, 158.8 (d_{C-F}, J = 258.3 Hz) 150.7, 146.2 (d_{C-F}, J = 4.0 Hz), 141.5, 138.0 (d_{C-F}, J = 24.4 Hz), 136.4, 131.6, 128.2, 125.9, 123.5 (d_{C-F}, J = 18.9 Hz), 123.2 (d_{C-F}, J = 4.3 Hz), 119.0, 112.4, 110.9, 101.4, 26.5, 26.0, 19.1, 18.4, −4.2. IR (film): ν (cm^{-1}) 3292, 2951, 2929, 2884, 2857, 1763, 1703, 1625, 1579, 1530, 1477, 1376, 1312, 1266, 1231, 1214, 1178, 1086, 1056, 970, 894, 842, 826, 801, 780, 750. HRMS calcd for $C_{29}H_{37}BrFN_3NaO_3Si_2$ (M + Na)$^+$ 652.1439, found (M + Na)$^+$ 652.1415.

Compound 4a. An orange solution of **14a** (300 mg, 0.601 mmol) in toluene (250 mL) was irradiated with a medium pressure Hg lamp using a uranium filter (50% transmission at 350 nm) for 3 hours with constant argon flow through the solution. The resulting orange suspension was concentrated to dryness *in vacuo*, adsorbed onto silica gel and subjected to silica gel chromatography with hexanes–EtOAc (8 : 1). The combined product eluents were dried *in vacuo* to provide **4a** (179 mg, 71%) as a yellow solid. ^{1}H NMR (360 MHz, CDCl$_3$): δ (ppm) 9.86 (s, 1H), 9.06 (m, 2H), 8.89 (d, J = 2.8 Hz, 1H), 7.65 (d, J = 8.0 Hz, 1H), 7.59 (t, J = 7.6 Hz, 1H), 7.45 (t, J = 7.4 Hz, 1H), 1.07 (s, 9H), 0.64 (s, 6H). ^{13}C NMR (90 MHz, CDCl$_3$): δ (ppm) 175.4, 174.2, 158.1 (d_{C-F}, J = 258.4 Hz), 141.8 (d_{C-F}, J = 27.8 Hz), 140.3, 139.5, 135.4, 131.8, 127.7, 125.8, 122.5, 122.4, 122.2, 120.4, (d_{C-F}, J = 5.1 Hz), 117.9 (d_{C-F}, J = 19.3 Hz), 115.0, 111.6, 26.7, 19.4, −3.8. IR (film): ν (cm^{-1}) 3454, 2926, 2856, 1748, 1692, 1615, 1561, 1524, 1464, 1418, 1401, 1363, 1339, 1303, 1257, 1234, 1216, 1183, 1062, 1043, 1006, 938, 898, 850, 828, 768. HRMS calcd for $C_{23}H_{21}FN_3O_2Si$ (M − H)$^-$ 418.1387, found (M − H)$^-$ 418.1397.

Compound 4j. An orange solution of **14j** (300 mg, 0.477 mmol) in toluene (250 mL) was irradiated with a medium pressure Hg lamp using a uranium filter (50% transmission at 350 nm) for 3 hours with constant argon flow through the solution. The resulting red solution was concentrated to dryness *in vacuo* and the experiment was repeated (200 mg, 0.318 mmol). The combined crude material was adsorbed onto silica gel and subjected to silica gel chromatography with hexanes–EtOAc (8 : 1). The combined product eluents were dried *in vacuo* to provide **4j** (320 mg, 73%) as a yellow solid. ^{1}H NMR (360 MHz, CDCl$_3$): δ (ppm) 9.86 (s, 1H), 9.03 (dd, J = 9.4, 2.9, 1H), 8.84 (d, J = 2.9, 1H), 8.58 (d, J = 2.5, 1H), 7.46 (dd, J = 8.2, 0.5, 1H), 7.14 (dd, J = 8.7, 2.5, 1H), 1.07 (s, 18H), 0.64 (s, 6H), 0.33 (s, 6H). ^{13}C NMR (90 MHz, CDCl$_3$): δ (ppm) 175.4, 173.8, 158.0 (d$_{C-F}$, J = 258.1 Hz) 151.2, 141.6, 141.3, 140.8, 135.5, 134.7, 131.9, 123.2, 122.7 (d$_{C-F}$, J = 7.1 Hz), 121.5, 119.8 (d$_{C-F}$, J = 4.8 Hz), 117.9 (d$_{C-F}$, J = 19.2 Hz), 114.9, 112.0, 26.7, 26.1, 19.3, 18.6, −3.8, −4.1. IR (film): ν (cm^{-1}) 3457, 3078, 2955, 2930, 2890, 2858, 1751, 1695, 1631, 1612, 1576, 1562, 1527, 1494, 1471, 1418, 1363, 1336, 1309, 1282, 1257, 1215, 1186, 1164, 1063, 1041, 1006, 966, 899, 884, 828, 814, 781, 769. HRMS calcd for C$_{29}$H$_{35}$FN$_3$O$_3$Si$_2$ (M − H)$^-$ 548.2201, found (M − H)$^-$ 548.2194.

Compound 15a. A suspension of ligand **4a** (20 mg, 0.048 mmol), [RuCp(CO)(CH$_3$CN)$_2$]$^+$PF$_6$$^-$ (30 mg, 0.072 mmol) and K$_2$CO$_3$ (7.3 mg, 0.053 mmol) in CH$_3$CN–CH$_3$OH (3 : 1) (2 mL) was stirred at room temperature overnight. The resulting dark purple reaction mixture was concentrated to dryness *in vacuo*, adsorbed onto silica gel and subjected to silica gel chromatography with hexanes–EtOAc (6 : 1). The combined product eluents were dried *in vacuo* to provide **15a** (19 mg, 66%) as a dark red film. ^{1}H NMR (360 MHz, CDCl$_3$): δ (ppm) 8.98 (dd, J = 9.3, 2.3 Hz, 1H), 8.89 (d, J = 8.0 Hz, 1H), 8.86 (br, 1H), 7.58 (t, J = 7.5 Hz, 1H), 7.46 (d, J = 8.1 Hz, 1H), 7.41 (t, J = 7.5 Hz, 1H), 5.23 (s, 5H), 1.06 (s, 9H), 0.63 (s, 6H). ^{13}C NMR (90 MHz, CDCl$_3$): δ (ppm) 199.2, 175.4, 174.8, 157.2 (d$_{C-F}$, J = 250.8 Hz), 155.3, 153.5, 144.5 (d$_{C-F}$, J = 33.9 Hz), 142.4, 133.9, 126.5, 125.8, 124.3, 121.7 (d$_{C-F}$, J = 8.5 Hz), 120.4, 119.3 (d$_{C-F}$, J = 20.0 Hz), 115.6, 115.3, 113.8 (d$_{C-F}$, J = 4.9 Hz), 80.7, 26.7, 19.4, −3.7. IR (film): ν (cm^{-1}) 3107, 2955, 2929, 2856, 1961, 1744, 1686, 1559, 1519, 1502, 1469, 1342, 1306, 1257, 1225, 1204, 1046, 1007, 908, 828, 745. HRMS calcd for C$_{29}$H$_{27}$FN$_3$O$_3$RuSi (M + H)$^+$ 614.0849, found (M + H)$^+$ 614.0839.

Compound 15j. A suspension of ligand **4j** (30 mg, 0.055 mmol), [RuCp(CO)(CH$_3$CN)$_2$]$^+$PF$_6$$^-$ (26 mg, 0.062 mmol) and K$_2$CO$_3$ (8.6 mg, 0.062 mmol) in CH$_3$CN–CH$_3$OH (3 : 1) (3 mL) was stirred at room temperature overnight. The resulting dark purple reaction mixture was concentrated to dryness *in vacuo*, adsorbed onto silica gel and subjected to silica gel chromatography with hexanes–EtOAc (8 : 1). The combined product eluents were dried *in vacuo* to provide **15j** (33 mg, 80%) as a purple film. ^{1}H NMR (360 MHz, CDCl$_3$): δ (ppm) 8.94 (dd, J = 9.4, 2.4 Hz, 1H), 8.80 (t, J = 2.4 Hz, 1H), 8.37 (d, J = 2.3 Hz, 1H), 7.30 (d, J = 8.7 Hz, 1H), 7.14 (dd, J = 8.7, 2.5 Hz, 1H), 5.22 (s, 5H), 1.07 (s, 9H), 1.05 (s, 9H), 0.62 (s, 6H), 0.32 (s, 6H). ^{13}C NMR (90 MHz, CDCl$_3$): δ (ppm) 199.2, 175.5, 174.4, 157.1 (d$_{C-F}$, J = 250.3 Hz), 155.4, 150.3, 148.8, 144.0 (d$_{C-F}$, J = 33.8 Hz), 142.8, 134.1, 124.8, 121.7 (d$_{C-F}$, J = 8.4 Hz), 120.5, 119.2 (d$_{C-F}$, J = 20.1 Hz), 115.4, 114.7, 113.0 (d$_{C-F}$, J = 4.7 Hz), 80.7, 29.9, 26.8, 19.3, 18.6, −3.7, −4.0. IR (film): ν (cm^{-1}) 3111, 2954, 2931, 2891, 2858, 1965, 1744, 1687, 1592, 1559, 1504, 1461, 1412, 1332, 1305, 1258, 1231, 1199, 1142, 1043, 1006, 973, 948, 908, 830, 778, 734. HRMS calcd for C$_{35}$H$_{41}$FN$_3$O$_4$RuSi$_2$ (M + H)$^+$ 744.1662, found (M + H)$^+$ 744.1658.

Compound 3a. A solution of **15a** (19 mg, 0.031 mmol) in CH$_2$Cl$_2$ (2 mL) was purged with argon while cooling to 0 °C. To the solution was added tetrabutylammonium fluoride (1 M solution in THF) (46 μL, 0.046 mmol) and the reaction mixture was allowed to slowly warm to room temperature. The resulting dark red reaction mixture was cooled to 0 °C and glacial acetic acid (2.6 μL, 0.046 mmol) was added, allowed to warm to room temperature and concentrated to dryness *in vacuo*. The crude material was subjected to silica gel chromatography with hexanes–EtOAc (3 : 1). The combined product eluents were dried *in vacuo* to provide **3a** (10 mg, 67%) as a purple solid. ^{1}H NMR (360 MHz, DMSO-d_6): δ (ppm) 11.13 (s, 1H), 9.51 (t, J = 2.5 Hz, 1H), 8.76 (dd, J = 9.4, 2.3 Hz, 1H), 8.64 (d, J = 7.7 Hz, 1H), 7.61 (d, J = 8.1 Hz, 1H), 7.54 (ddd, J = 8.1, 6.9, 1.2 Hz, 1H), 7.35 (ddd, J = 7.9, 6.8, 1.0 Hz, 1H), 5.55 (s, 5H). ^{13}C NMR (90 MHz, DMSO-d_6): δ (ppm) 200.5, 170.5, 170.2, 156.7 (d$_{C-F}$, J = 248.9 Hz), 154.1, 152.8, 146.4 (d$_{C-F}$, J = 34.2 Hz), 141.1, 131.4, 126.1, 123.9, 123.4, 120.5 (d$_{C-F}$, J = 8.6 Hz), 119.7, 117.3 (d$_{C-F}$, J = 20.2 Hz), 115.8, 114.3, 111.7 (d$_{C-F}$, J = 4.9 Hz), 81.7. IR (film): ν (cm^{-1}) 1954, 1743, 1692, 1564, 1523, 1494, 1464, 1407, 1338, 1292, 1255, 1223, 1199, 1105, 1066, 987. HRMS calcd for C$_{23}$H$_{13}$FN$_3$O$_3$Ru (M + H)$^+$ 499.9984, found (M + H)$^+$ 499.9978.

Compound 3j. A solution of **15j** (21 mg, 0.028 mmol) in CH$_2$Cl$_2$ (2 mL) was purged with argon while cooling to 0 °C. To the solution was added tetrabutylammonium fluoride (1 M solution in THF) (70 μL, 0.070 mmol) and the reaction mixture was allowed to slowly warm to room temperature. The resulting dark blue reaction mixture was cooled to 0 °C and glacial acetic acid (4.0 μL, 0.070 mmol) was added, allowed to warm to room temperature and concentrated to dryness *in vacuo*. The crude material was subjected to silica gel chromatography with CH$_2$Cl$_2$–CH$_3$OH (50 : 1 to 35 : 1). The combined product eluents were dried *in vacuo* to provide **3j** (14 mg, 100%) as a blue-green solid. ^{1}H NMR (500 MHz, DMSO-d_6): δ (ppm) 11.01 (s, 1H), 9.42 (t, J = 2.6, 1H), 9.17 (s, 1H), 8.71 (dd, J = 9.4, 2.4, 1H), 8.08 (d, J = 2.5, 1H), 7.43 (d, J = 8.7, 1H), 7.07 (dd, J = 8.7, 2.5, 1H), 5.52 (s, 5H). ^{13}C NMR (125 MHz, DMSO-d_6): δ (ppm) 200.4, 170.4, 170.3, 156.5 (d$_{C-F}$, J = 248.4 Hz), 153.9, 151.7, 147.0, 145.5 (d$_{C-F}$, J = 34.3 Hz), 141.5, 131.7, 123.8, 120.5 (d$_{C-F}$, J = 8.7 Hz), 117.2, 117.0, 116.2 (d$_{C-F}$, J = 18.2 Hz), 114.8, 110.2 (d$_{C-F}$, J = 4.6 Hz), 108.3, 81.6. IR (film): ν (cm^{-1}) 3445, 3278, 2922, 1953, 1750, 1710, 1592, 1556, 1502, 1472, 1408, 1336, 1260, 1207, 1056, 1022, 997, 936, 924, 872, 807, 773, 700. HRMS calcd for C$_{23}$H$_{13}$FN$_3$O$_4$Ru (M + H)$^+$ 515.9933, found (M + H)$^+$ 515.9927.

Protein kinase assays

Protein kinases (human) and substrates were purchased from Upstate Biotechnology USA. Ten nM concentrations of stuarosporine, **1**, **2** and **3a–p** were incubated at room temperature in 20 nM MOPS, 30 mM MgCl$_2$, 0.8 μg μL^{-1} BSA, 5% DMSO (resulting from the inhibitor stock solution), pH 7.0, in the presence of substrate (GSK-3α: 20 μM phosphoglycogen synthase peptide-2; Pim-1: 50 μM S6 kinase/Rsk2 substrate peptide 2) and

This journal is © The Royal Society of Chemistry 2007

Org. Biomol. Chem., 2007, **5**, 1218–1227 | 1225

kinase (experiments in Fig. 2: 0.9 nM GSK-3α, 0.8 nM Pim-1; experiments in Fig. 3: 0.1 nM GSK-3α). After 15 minutes, the reaction was initiated by adding ATP to a final concentration of 100 μM, including approximately 0.2 μCi μL^{-1} [γ-^{32}P]ATP. Reactions were performed in a total volume of 25 μL. After 30 minutes, the reaction was terminated by spotting 17.5 μL on a circular P81 phosphocellulose paper (2.1 cm diameter, Whatman), followed by washing four times (5 minutes each wash) with 0.75% phosphoric acid and once with acetone. The dried P81 papers were transferred to a scintillation vial, and 5 mL of scintillation cocktail was added, and the counts per minute (CPM) were determined with a Beckmann 6000 scintillation counter. IC$_{50}$ values were defined to be the concentration of inhibitor at which the CPM was 50% of the control sample, corrected by the background.

Protein expression, purification and crystallization

The plasmid encoding full-length Pim-1 (gi33304198) was a generous gift from Dr S. Knapp, Oxford University, Centre for Structural Genomics Botnar Research Centre, UK. The protein was expressed and purified as described previously.[18] Briefly, expression of protein in BL21(DE3)pLysS cells was induced with 2 mM IPTG for 5 hours at 18 °C. Cells were collected by centrifugation, resuspended in 50 mM HEPES pH 7.5, 500 mM NaCl, 5% glycerol, and lysed applying high pressure (French-press). The lysate was purified with DEAE cellulose column (DE52 Whatmann) and Ni-NTA chromatography (Qiagen). The protein was treated overnight with lambda phosphatase and TEV protease to remove phosphate and His$_6$-tag respectively. Further purification was achieved with a mono-Q column (Amersham-Biosiences), which separated dephosphorylated and phosphorylated fractions, and an additional Ni-NTA affinity column to obtain high purity. Separated dephosphorylated and phosphorylated fractions were concentrated to 5 mg mL^{-1} in crystallography buffer, 50 mM HEPES pH 7.5, 250 mM NaCl, 5% glycerol, 10 mM DTT. Ruthenium complex was added to the protein from 10 mM DMSO stock solution to the final concentration of 1 mM. Crystals of nonphosphorylated Pim-1 with (S)-3a were grown at 4 °C in 4 μL sitting drops where 2 μL of protein solution was mixed with 2 μL of the precipitate stock containing 0.2 M magnesium chloride, 100 mM BisTrisPropane (pH 6.5), 20% PEG3350, 10% ethylene glycol and 0.3% DMSO.

Data collection and structure determination

Cryoprotected crystals yielded X-ray diffraction to 2.2 Å on a Rigaku RU-200HB rotating anode X-ray generator equipped with R-axis IV++ image plate detector. Diffraction data were indexed and merged using the program Crystal Clear (d*Trek).[19] The structure was determined by difference Fourier technique using a structure of Pim-1 (PDB code 2BZI; inhibitor, solvent, and ions were removed) as an initial model for phasing.[6] Iterative cycles of refinement and manual rebuilding of the model were performed using the program REFMAC5 and O, respectively.[20,21] Data collection and refinement statistics are listed in Table 2. Coordinates for the structure have been deposited in the Protein Data Bank (PDB code 2OI4).

Table 2 Crystallographic data and refinement statistics[a]

Space group	$P6_5$
Cell dimension/Å	$a,b = 98.10$, $c = 80.67$
Resolution/Å	2.2
Total observations (unique, redundancy)	57076 (20939, 2.7)
Completeness (outer shell) [%]	93.1 (96.4)
R_{merge} (outer shell)	0.104 (0.450)
I/σ	6.2
R_{work} (R_{free})	0.189 (0.245)
Rmsd bond length/Å	0.019
Rmsd bond angle/°	1.89

[a] Rmsd = root mean square deviation.

Cyclic voltammetry

Voltammetric experiments were conducted with a computer controlled Eco Chemie μAutolab III potentiostat with 1 mm diameter planar Pt and glassy carbon (GC) working electrodes, a Pt wire auxiliary electrode and an Ag wire reference electrode (isolated by a salt bridge containing 0.5 M Bu$_4$NPF$_6$ in CH$_3$CN). Potentials were referenced to the ferrocene/ferrocenium redox couple. The electrochemical cell was thermostatted at 293 K using and Eyela PSL-1000 variable temperature cooling bath. Data were obtained at a scan rate of 1 V s^{-1} in CH$_2$Cl$_2$ with 0.25 M Bu$_4$NPF$_6$ as the supporting electrolyte. Oxidative peak potentials (E_p^{ox}): **1** = +0.54 V, **2** = ca. +0.36 V, **3a** = +0.60 V.

References

1 For bioorganometallic and medicinal organometallic chemistry, see: K. Severin, R. Bergs and W. Beck, *Angew. Chem., Int. Ed.*, 1998, **37**, 1634–1654; D. B. Grotjahn, *Coord. Chem. Rev.*, 1999, **190**, 1125–1141; special issue of *J. Organomet. Chem.*, ed. G. Jaouen, 1999, **589**, 1–126; N. Metzler-Nolte, *Angew. Chem., Int. Ed.*, 2001, **40**, 1040–1043; R. H. Fish and G. Jaouen, *Organometallics*, 2003, **22**, 2166–2177; R. Stodt, S. Gencaslan, I. M. Müller and W. S. Sheldrick, *Eur. J. Inorg. Chem.*, 2003, 1873–1882; D. Schlawe, A. Majdalani, J. Velcicky, E. Heßler, T. Wieder, A. Prokop and H.-G. Schmalz, *Angew. Chem., Int. Ed.*, 2004, **43**, 1731–1734; D. R. van Staveren and N. Metzler-Nolte, *Chem. Rev.*, 2004, **104**, 5931–5985; I. Ott, B. Kircher and R. Gust, *J. Inorg. Biochem.*, 2004, 485–489; *Bioorganometallics*, ed. G. Jaouen, Wiley-VCH, Weinheim, 2005; Y. K. Yan, M. Melchart, A. Habtemariam and P. J. Sadler, *Chem. Commun.*, 2005, 4764–4776; P. J. Dyson and G. Sava, *Dalton Trans.*, 2006, 1929–1933; U. Schatzschneider and N. Metzler-Nolte, *Angew. Chem., Int. Ed.*, 2006, **45**, 1504–1507.

1226 | *Org. Biomol. Chem.*, 2007, **5**, 1218–1227

This journal is © The Royal Society of Chemistry 2007

2 H. Bregman, D. S. Williams, G. E. Atilla, P. J. Carroll and E. Meggers, *J. Am. Chem. Soc.*, 2004, **126**, 13594–13595.

3 D. S. Williams, G. E. Atilla, H. Bregman, A. Arzoumanian, P. S. Klein and E. Meggers, *Angew. Chem., Int. Ed.*, 2005, **44**, 1984–1987.

4 H. Bregman, D. S. Williams and E. Meggers, *Synthesis*, 2005, 1521–1527.

5 H. Bregman, P. J. Carroll and E. Meggers, *J. Am. Chem. Soc.*, 2006, **128**, 877–884.

6 J. É. Debreczeni, A. N. Bullock, G. E. Atilla, D. S. Williams, H. Bregman, S. Knapp and E. Meggers, *Angew. Chem., Int. Ed.*, 2006, **45**, 1580–1585.

7 G. E. Atilla-Gokcumen, D. S. Williams, H. Bregman, N. Pagano and E. Meggers, *ChemBioChem*, 2006, **7**, 1443–1450.

8 H. Bregman and E. Meggers, *Org. Lett.*, 2006, **8**, 5465–5468.

9 For co-crystal structures of staurosporine with protein kinases, see for example: L. M. Toledo and N. B. Lydon, *Structure*, 1997, **5**, 1551–1556; A. M. Lawrie, M. E. M. Noble, P. Tunnah, N. R. Brown, L. N. Johnson and J. A. Endicott, *Nat. Struct. Biol.*, 1997, **4**, 796–801; L. Prade, R. A. Engh, A. Girod, V. Kinzel, R. Huber and D. Bossemeyer, *Structure*, 1997, **5**, 1627–1637.

10 C. B. de Koning, J. P. Michael and A. L. Rousseau, *J. Chem. Soc., Perkin Trans. 1*, 2000, 1705–1713.

11 E. Vazquez, I. W. Davies and J. F. Payack, *J. Org. Chem.*, 2000, **67**, 7551–7552.

12 E. Vedejs, R. W. Chapman, S. C. Fields, S. Lin and M. R. Schrimpf, *J. Org. Chem.*, 1995, **60**, 3020–3027.

13 T. Apelqvist and D. Wensbo, *Tetrahedron Lett.*, 1996, **37**, 1471–1472.

14 T. Yoshida, M. Nishiyachi, N. Nakashima, M. Murase and E. Kotani, *Chem. Pharm. Bull.*, 2002, **50**, 872–876; T. Yoshida, M. Nishiyachi, N. Nakashima, M. Murase and E. Kotani, *Chem. Pharm. Bull.*, 2003, **51**, 209–214.

15 The absolute configuration at the ruthenium has been assigned according to the priority order of the ligands being η^5-C_5H_5 > pyridine [N=C, C, C)] > indole [N=C, C, lone pair)] > CO.

16 S. S. Taylor and E. Radzio-Andzelem, *Structure*, 1994, **2**, 345–355.

17 M. D. Jacobs, J. Black, O. Futer, L. Swenson, B. Hare, M. Fleming and K. Saxena, *J. Biol. Chem.*, 2005, **280**, 13728–13734.

18 A. N. Bullock, J. É. Debreczeni, O. Y. Fedorov, A. Nelson, B. D. Marsden and S. Knapp, *J. Med. Chem.*, 2005, **48**, 7604–7614.

19 J. W. Pflugrath, *Acta Crystallogr., Sect. D*, 1999, **55**, 1718–1725.

20 G. N. Murshudov, A. A. Vagin and E. J. Dodson, *Acta Crystallogr., Sect. D*, 1997, **53**, 240–255.

21 T. A. Jones, J. Y. Zou, S. W. Cowan and M. Kjeldgaard, *Acta Crystallogr., Sect. A*, 1991, **47**, 110–119.

This journal is © The Royal Society of Chemistry 2007

Org. Biomol. Chem., 2007, **5**, 1218–1227 | 1227